

# Insights into the faithful translation of the genetic code by the ribosome

Sean P. McClory<sup>\*†</sup>

## Introduction

In all life, genetic information is stored in the form of deoxy-ribonucleic acids (DNA), and in response to various stimuli, genes are transcribed from DNA into a messenger ribonucleic acid (mRNA) and then translated into proteins, which carry out many important functions of the cell. It is critical that each step of this process (DNA synthesis, transcription, and translation) occur with high accuracy to ensure that the resulting gene products do not contain numerous errors. Because of this, the enzymes that are responsible for each step have evolved complex mechanisms to maintain the fidelity of their work. The details of these mechanisms are of great interest, not only because they are critical for life, but also because defects in them can cause disease or be exploited to fight harmful microbes.

Translation, where the genetic information encoded in an mRNA directs the synthesis of a protein, occurs on large complexes of both RNA and protein called ribosomes<sup>1,2</sup>. Each ribosome is composed of 2 subunits. In bacteria, these are the large 50S subunit and the small 30S subunit. The ribosome contains 3 transfer-RNA (tRNA) binding sites termed A (aminoacyl), P (peptidyl) and E (exit), and a binding site for the mRNA within the 30S subunit<sup>1</sup>. Each mRNA is organized into 3-nucleic-acid codons, each specific for one of the 20 amino-acids present in all organisms or a “stop” which signifies the end of a gene (Table 1). Every amino-acid added to the growing protein is delivered to the ribosome by an aminoacyl-tRNA (aa-tRNA) in complex with elongation

---

<sup>\*</sup> The research presented below has been published in *RNA* **16**, 1925-1934 (2010).

<sup>†</sup> Joshua Leisring, Daoming Qin, and Kurt Fredrick also contributed to this work.

factor (EF)-Tu and GTP (Fig 1). The anticodon end of the aa-tRNA binds the codon being translated in the A site, which leads to GTP hydrolysis by EF-Tu. This event causes EF-Tu to release the aa-tRNA into the A site, where the ribosome catalyzes the transfer of the growing protein from the P site tRNA to the aa-tRNA in the A site. Subsequently the mRNA and two tRNAs undergo translocation in a stepwise manner one codon from the P to the E site and from A to P, which is catalyzed by the factor EF-G. Dissociation of the tRNA from the E site results in a ribosome containing a peptidyl-tRNA one amino-acid longer ready to undergo another elongation cycle (Fig 1)<sup>1-3</sup>.

In order to ensure that each residue in the growing protein is accurately synthesized, the ribosome must select the cognate (correct) aa-tRNA for each codon translated. This selection primarily depends on base pairing between the codon and the tRNA anticodon<sup>1,3</sup>. However, many near-cognate tRNAs are able to form partial base pairs with the codon. During translation, these near-cognate tRNA compete with cognate tRNA for the ribosome's A-site, and for most codons the near-cognate species vastly outnumber the cognate tRNAs carrying the correct amino acid<sup>4</sup>.

To overcome this challenge, the ribosome employs a two-phase selection mechanism (Fig 2). Following initial binding of the aa-tRNA•EF-Tu•GTP ternary complex to the ribosome, the aa-tRNA anticodon binds to the codon in the A-site. Codon recognition triggers GTP hydrolysis by EF-Tu, after which EF-Tu undergoes a conformational change to the GDP bound form and releases the aa-tRNA into the ribosome. To reach the peptidyl transfer center, the aa-tRNA must undergo accommodation, moving from EF-Tu bound A/T state to the A/A state fully within the A-site. During aa-tRNA selection, incorrect tRNAs can dissociate from the codon

recognition complex during initial selection, or before accommodation during the proofreading phase<sup>1,3,5</sup>. Codon-anticodon binding slows dissociation of cognate tRNAs during these two steps, but the ribosome also couples the energy of codon-anticodon pairing to the forward steps of GTP hydrolysis and accommodation, so that cognate aa-tRNAs are rapidly incorporated into the ribosome, while near-cognate tRNAs are efficiently rejected<sup>5</sup>. This induced fit mechanism suggests that the ribosome undergoes a conformational change in response to cognate aa-tRNA changing from an inactive to an active form.

Clues to the structural nature of the induced fit mechanism of aa-tRNA selection have come from X-ray crystallography structures of isolated 30S subunits with cognate or near-cognate anticodon stem-loops (ASLs) bound in the A-site. In the presence of cognate tRNA, two universally conserved adenosines, A1492 and A1493, flip out from helix h44 in the A-site, and dock into the minor groove of the codon-anticodon mini-helix, an interaction that is specific for the Watson-Crick geometry of a cognate pairing. Additionally, these cognate complexes display a global conformational change where the head and shoulder domains of the ribosome rotate inward toward the platform. Neither of these conformational changes was observed in crystals bound with near-cognate ASLs. Therefore, it was suggested that the head and shoulder movement, described as “domain closure”, may play a critical role in the induced fit mechanism of aa-tRNA selection<sup>6</sup>.

However, while these crystal structures provide many important clues to the nature of the selection mechanism, they are limited in that they only give still images of what must be a dynamic process during translation. X-ray crystallography studies neither directly link the domain closure rearrangement to aa-tRNA selection, nor answer several

important questions about the process, such as: how does codon recognition in the A-site stimulate GTP hydrolysis in the EF-Tu active site, over 75Å away?

To address these questions, we have taken a genetic approach to isolate point mutations within the 16S rRNA component of the 30S subunit, which disrupt the ribosome's ability to correctly selection aa-tRNA during translation. These mutations point to specific functions in aa-tRNA selection for distinct regions of the ribosome. Additionally, we show how several of these mutations affect aa-tRNA selection *in vitro* in order to demonstrate how they affect the dynamics of the selection mechanism.

## **Results and Discussion**

### **Isolation of 16S rRNA mutations causing errors during aa-tRNA selection**

Genetic studies of ribosomal RNA are complicated by two factors. One, there are multiple copies of the rRNA genes within the cell, *E. coli* has 7, making difficult to create a homogeneous population of mutant ribosomes<sup>7</sup>. Secondly, ribosome mutations can affect the expression of many genes in a cell, which can lead to secondary phenotypes not directly related to the ribosome itself. To circumvent these difficulties, we used a specialized ribosome system, which takes advantage of the fact that in bacteria, the Shine-Dalgarno (SD) sequence directs the ribosome to the start codon of a gene by directly interacting with the anti-Shine-Dalgarno (ASD) region of the 16S rRNA<sup>8,9</sup>.

In this specialized ribosome system (described previously REF), plasmid pKF207 is used to express a 16S rRNA gene containing a mutation of the ASD region (ASD\*: 5'-GGGGU-3'). Ribosomes generated within the cell specifically translate a chromosomally encoded *lacZ* reporter gene with a corresponding mutant SD sequence (SD\*:5'-AUCCC-3'). This ensures that additional 16S rRNA mutations in pKF207 do

not affect the expression of endogenous genes in the cell and that the *lacZ* reporter is not translated by endogenous wild-type ribosomes.

To identify mutations that affect the ribosome's ability to correctly select aa-tRNA, we employed two constructs of the *lacZ*(SD\*) reporter gene. The first, strain KLF4001, contains a missense mutation at a critical glutamate codon, codon 461 GAA (Glu) to GAT (Asp). Expression of the active *lacZ* gene product,  $\beta$ -galactosidase, requires the ribosome to suppress the missense mutation by translating the GAU aspartate codon with a Glu-tRNA. The second construct, KLF2723, contains a nonsense mutation where codon 585 of *lacZ* has been replaced by a premature stop codon, TGA. In this strain, active  $\beta$ -galactosidase expression requires that the codon be mis-read by an aa-tRNA rather than the release factor RF2 that is typically responsible for ending translation at UGA codons. Plasmid pKF207 was randomly mutagenized and transformed into either KLF4001 or KLF2723. Transformants were screened for increased  $\beta$ -galactosidase expression by growth on X-gal plates. Mutations causing mis-translation were identified by sequencing pKF207 (Table 2)<sup>7</sup>.

Mutations identified in the genetic screen were introduced *de novo* into pKF207 by site directed mutagenesis and transformed into either KLF4001 or KLF2723 to confirm their phenotypes. The effects of these mutations, along with a number of additional mutations, on translation fidelity *in vivo* was then quantified (Fig 3) by comparing the relative expression of  $\beta$ -galactosidase from KLF4001 between mutant and WT pKF207 16S rRNA<sup>7</sup>.

### **Elements of 16S rRNA involved in aa-tRNA selection**

Mutations isolated by genetic screen cluster in distinct regions of the 30S structure (Fig 4) implicating these residues in the mechanism of aa-tRNA selection. Notably, these mutations additionally appear to cluster in areas where the 30S shoulder domain interacts with other regions of the ribosome. These observations provide additional insights previous biochemical and genetic studies.

The mutations with the strongest phenotypes in both the missense suppression and nonsense suppression screens were located within the 30S A-site, where codon recognition takes place (Fig 5A). These mutations likely exert their effects by modulating how the codon and anticodon interact. In fact, mutations at C1054 may have effects specific to the aa-tRNA being translated. This residue forms a direct interaction with the 3<sup>rd</sup> position of the tRNA anticodon. Mutations of this residue to any of the 3 other nucleic acids (A, G, or U) all significantly increased nonsense suppression in KLF2723. However, while C1054A and C1054G increased missense suppression in KLF4001 by 20- and 40-fold respectively, C1054U appeared to *decrease* translation errors in this strain<sup>7</sup>. This may be due to the fact that codon 461 in the KLF4001 *lacZ* gene must be misread by Glu-tRNA<sup>Glu</sup>, while codon 585 in the KLF2723 *lacZ* is likely misread by Trp-tRNA<sup>Trp</sup>. Alternatively, these residue specific defects may reflect specific interactions between residue 1054 and RF2, which normally reads the premature stop codon in KLF2723.

Several mutations were located near proteins S4 and S5 on the solvent exposed side of the 30S (Fig 5B). The strongest of these was a G299A mutation in helix h12 (Table 2) which increased translation errors by nearly 10-fold (Fig 3). H12 is located near the interface of S4 and S5. Protein S4 is part of the 30S shoulder domain, while S5 is

located within the 30S platform. These proteins form an interaction with one another, however, during domain closure, several salt bridges between the proteins are broken and the proteins separate slightly<sup>6</sup>. Mutations in h12 likely further destabilize the interface of the shoulder and platform domains and promote inward shoulder rotation. In fact, G299 appears to pair with the hoogsteen face of G566, stabilizing several sharp turns in the 16S rRNA at the domain interface (Fig 5B). This observation is highly suggestive that the domain closure movement observed in crystal structures plays an important role in aa-tRNA selection. Three more mutations, U598C, G606A, and C634U, are located within h21 (Table 2), a helix which spans the solvent face of the ribosome connecting the shoulder and platform domains (Fig 5B). These mutations likely additionally destabilize the shoulder and promote domain closure. Further supporting this idea are three mutations  $\Delta$ U420, G423A, and G424A, in h16 (Table 2), which all disrupt the conserved UCGG tetraloop structure of this helix. The h16 tetraloop is located on the edge of the 30S shoulder and forms a contact with protein S3 in the 30S head domain (Fig 5C) in the open (empty or near-cognate ASL bound) 30S structure, a contact which is broken upon domain closure. These three separate clusters of mutations, taken together, strongly support a model where movement of the 30S shoulder plays an important role in aa-tRNA selection.

The largest cluster of mutations identified was found in either helix h8 or helix h14 (Table 2). These two helices form an interaction with each other, and the 50S subunit, forming bridge B8, near the binding site of EF-Tu (Fig 5C,D). The mutations with the strongest phenotypes were located at A160, A161, and G347, which form the

tertiary interaction between these helices, suggesting that destabilizing this interaction promotes translation errors.

### **The role of h8 and h14 in aa-tRNA selection**

Because of the significant distance of the h8/h14 region from the A-site, it is difficult to rationalize its direct role in aa-tRNA selection. However, a recent cryo-EM structure of the ribosome has suggested that h14 forms a direct contact with the switch 1 motif of EF-Tu during the initial selection phase of translation (Fig 5C, D)<sup>10</sup>. Switch 1 forms part of a hydrophobic gate to the GTPase active site of EF-Tu, preventing access of the H<sub>2</sub>O molecule necessary for GTP hydrolysis. The study's authors proposed that the h14 contact may be necessary to open the hydrophobic gate and activate EF-Tu for GTP hydrolysis, a theory that may explain the role of this region in aa-tRNA selection.

To test this hypothesis, we used site-directed mutagenesis to create 16S rRNAs where h14 is truncated by 1 to 2 base-pairs, and h8 is truncated by 2 to 3 base-pairs. All of these mutations are structurally predicted to prevent the association between EF-Tu switch 1 and either h14 or h8. *In vivo* all of these mutations supported significant levels of translation, at least 25% of wild type (Fig 3), which is not consistent with this h14 contact being essential for GTPase activation. However, all of these mutations were significantly error prone (Fig 3).

To further discern the role of this region in aa-tRNA selection, we purified ribosomes containing either a 2-base pair truncation of h14, a 3-base-pair truncation of h8 or a G347U mutation in h14 that was the strongest mutation in this region identified in the genetic screen, and measured the ability of these ribosomes to stimulate GTP hydrolysis by EF-Tu in single turnover *in vitro* translation assays. Surprisingly, we found



that each of these mutations increased the rate of GTP hydrolysis by Phe-tRNA<sup>Phe</sup>•EF-Tu•GTP translating either a cognate UUU codon or a near-cognate CUU codon. This effect was more pronounced in the case of CUU programmed ribosomes, meaning that these mutant ribosomes are more likely to allow near-cognate aa-tRNA through the initial selection phase than wild-type ribosomes, consistent with their error-prone phenotype *in vivo*.

These data are inconsistent with a model where h14 plays a role in activating EF-Tu for GTP hydrolysis, and, in fact, suggest that the h8/h14 region is responsible for negatively regulating this process. In light of this, and our data suggesting that domain closure of the 30S subunit plays a critical role in aa-tRNA selection, we propose a model where bridge B8, formed by contacts between h14 and 50S protein L19, acts to prevent 30S shoulder rotation from moving EF-Tu into contact with 50S elements that activate GTP hydrolysis (Fig 7). In this model, rearrangement of the 30S A-site in response to a cognate codon-anticodon pairing drives the inward rotation of the 30S shoulder, which moves EF-Tu into contact with elements of the 50S subunit activating GTP hydrolysis. Bridge B8 increases the energy barrier for shoulder rotation, increasing the selectivity of this step by preventing near-cognate complexes from inducing these 50S contacts. Mutations that destabilize this bridge increase miscoding by reducing this energy barrier.

## **Conclusion**

The results of our genetic screen have identified many novel mutations in the ribosome that disrupt the aa-tRNA selection process. Analysis of these mutations has allowed us to develop a model for this process that may explain several previous observations. These insights contribute to our understanding of this critical cellular

process and may present additional targets for novel antibiotics that inhibit decrease the fidelity of translation.

## **Materials and Methods**

### **Bacterial strains**

Indicator strains KLF4001, KLF2723, and KLF2674 carry the lacZ reporter in single copy on the chromosome and were constructed from parental strain CSH142 [F- ara  $\Delta$ (gpt-lac)5] as described previously <sup>8,9</sup>. In these strains, lacZ is preceded by the alternative Shine–Dalgarno (SD) sequence 5'-ATCCC-3' (SD\*) and is under transcriptional control of a consensus Pant promoter. In KLF4001, lacZ carries a missense mutation at codon 461 (GAA to GAT). In KLF2723, lacZ contains a UGA stop at codon 585. In KLF2674, lacZ contains no mutations (control strain). These indicator strains were made recA- by P1 transduction using donor strain JC14604 [ $\Delta$ (recA-srl)306, srlR301::Tn10] obtained from the E. coli Genetic Stock Center (Yale University). E. coli  $\Delta$ 7 prn strains were made using SQZ10 as described previously <sup>9</sup>.

### **Engineered mutations**

The precise nature of the deletion mutations constructed in 16S rRNA are as follows: h8 $\Delta$ 2bp,  $\Delta$ (154,155,166,167); h8 $\Delta$ 3bp,  $\Delta$ (154,155,157,164,166,167); h14 $\Delta$ 1bp,  $\Delta$ (340,349); h14 $\Delta$ 2bp,  $\Delta$ (340,341,348,349); h16 $\Delta$ 1bp,  $\Delta$ (418,425); and h16 $\Delta$ 2bp,  $\Delta$ (417,418,425,426). For the insertion mutations in h14, either one (h14ins1bp) or two (h14ins2bp) additional C–G pairs were added in the middle of the helix.

### **Genetic screens**

The genetic screens were performed as described previously<sup>11</sup>, except that indicator strains KLF4001 and KLF2723 were used. Mutator strain XL1-Red (Stratagene) was employed for the mutagenesis.

### **$\beta$ -Galactosidase assays**

$\beta$ -Galactosidase activity was measured as described previously<sup>8,9</sup>, using the substrate o-nitrophenyl- $\beta$ -D-galactopyranoside (ONPG; Sigma).

### **Kinetic assays**

GTP hydrolysis measurements were performed as described<sup>12</sup>, except that reactions were carried out in polymix buffer<sup>13</sup>. The mRNAs were the same as those used in a previous study<sup>14</sup>.

### **Acknowledgements**

The data presented above has been previously published in reference 7. We thank C. Squires and S. Quan for E. coli strain SQZ10 and J. Ling for providing purified mRNA. This work was supported by National Institutes of Health grant no. GM072528.

1. Schmeing, T.M. & Ramakrishnan, V. What recent ribosome structures have revealed about the mechanism of translation. *Nature* **461**, 1234-1242 (2009).
2. Shoji, S., Walker, S.E. & Fredrick, K. Ribosomal translocation: one step closer to the molecular mechanism. *ACS Chem. Biol* **4**, 93-107 (2009).
3. Zaher, H.S. & Green, R. Fidelity at the molecular level: lessons from protein synthesis. *Cell* **136**, 746-762 (2009).
4. Kramer, E.B. & Farabaugh, P.J. The frequency of translational misreading errors in E. coli is largely determined by tRNA competition. *RNA* **13**, 87-96 (2007).

5. Pape, T., Wintermeyer, W. & Rodnina, M. Induced fit in initial selection and proofreading of aminoacyl-tRNA on the ribosome. *EMBO J* **18**, 3800-3807 (1999).
6. Ogle, J.M., Murphy, F.V., Tarry, M.J. & Ramakrishnan, V. Selection of tRNA by the ribosome requires a transition from an open to a closed form. *Cell* **111**, 721-732 (2002).
7. McClory, S.P., Leisring, J.M., Qin, D. & Fredrick, K. Missense suppressor mutations in 16S rRNA reveal the importance of helices h8 and h14 in aminoacyl-tRNA selection. *RNA* **16**, 1925-1934 (2010).
8. Abdi, N.M. & Fredrick, K. Contribution of 16S rRNA nucleotides forming the 30S subunit A and P sites to translation in Escherichia coli. *RNA* **11**, 1624-1632 (2005).
9. Qin, D., Abdi, N.M. & Fredrick, K. Characterization of 16S rRNA mutations that decrease the fidelity of translation initiation. *RNA* **13**, 2348-2355 (2007).
10. Villa, E. et al. Ribosome-induced changes in elongation factor Tu conformation control GTP hydrolysis. *Proc. Natl. Acad. Sci. U.S.A* **106**, 1063-1068 (2009).
11. Qin, D. & Fredrick, K. Control of translation initiation involves a factor-induced rearrangement of helix 44 of 16S ribosomal RNA. *Mol. Microbiol* **71**, 1239-1249 (2009).
12. Ledoux, S. & Uhlenbeck, O.C. Different aa-tRNAs are selected uniformly on the ribosome. *Mol. Cell* **31**, 114-123 (2008).
13. Ehrenberg, M., Bilgin, N. & Kurland, C. Design and use of a fast and accurate in vitro translation system. *Ribosomes and protein synthesis (ed. Spedding, G)* 101-129 (1990).

14. Ling, J., Yadavalli, S.S. & Ibba, M. Phenylalanyl-tRNA synthetase editing defects result in efficient mistranslation of phenylalanine codons as tyrosine. *RNA* **13**, 1881-1886 (2007).

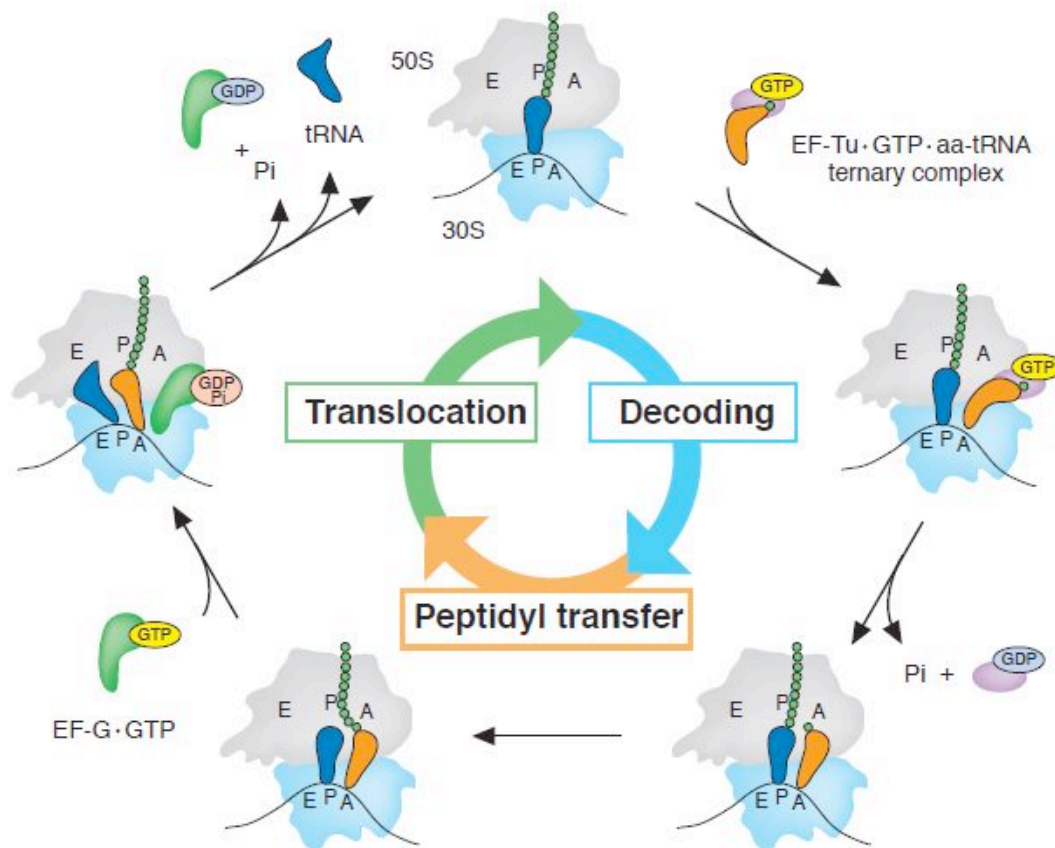


**Figure 1.** Scheme for a translation elongation cycle<sup>2</sup>. Each cycle of translation elongation is composed of three major steps: decoding, peptidyl transfer, and translocation. In decoding, aminoacyl-tRNA (aa-tRNA) is delivered to the A site as part of a ternary complex with EF-Tu and GTP. This is followed by rapid and functionally irreversible transfer of the peptidyl group from P-tRNA to A-tRNA. EF-G · GTP then catalyzes

translocation, the coupled movement of tRNA and mRNA in the ribosome. Deacylated tRNA dissociates from the E site before or during the next round of elongation.

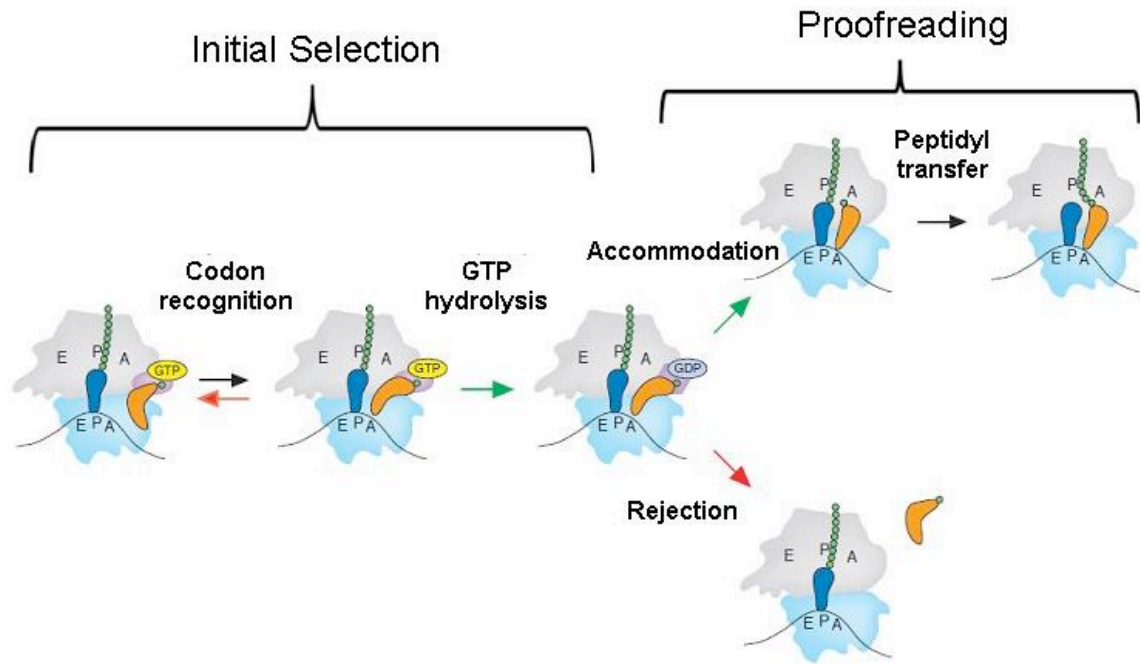


**Figure 2.** Scheme for aminoacyl-tRNA selection. Following the binding of the aa-tRNA•EF-Tu•GTP ternary complex to the ribosome, the tRNA anticodon is recognized in the A-site. This stimulates GTP hydrolysis, causing EF-Tu to release the aa-tRNA into the ribosome where it is either accommodated into the A site to undergo peptidyl transfer or is rejected from the ribosome. Green arrows represent steps that are stimulated by cognate aa-tRNA. Red arrows represent steps that are slowed by cognate aa-tRNA.

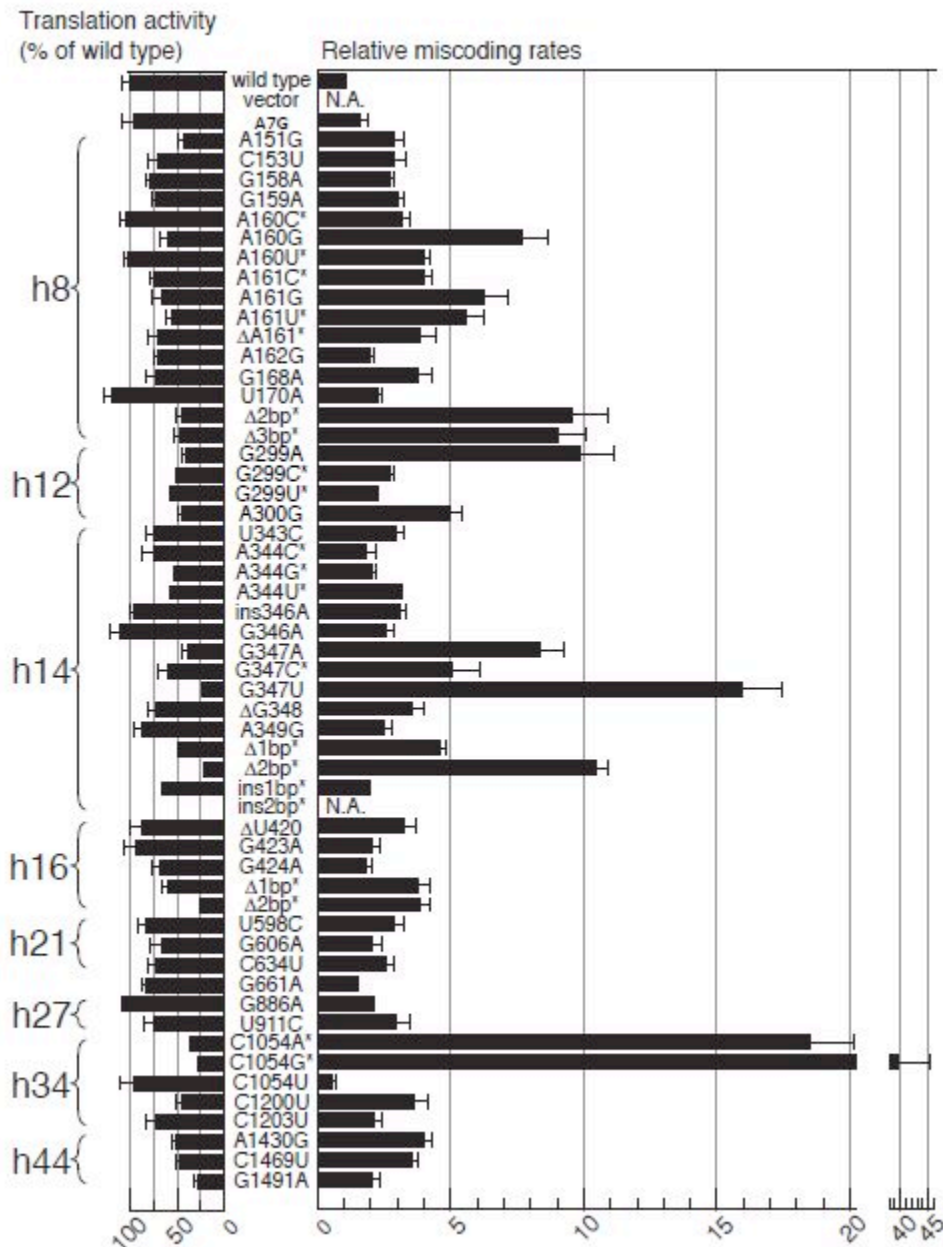


**Figure 3.** Effects of 16S rRNA mutations on missense suppression. Values on the leftward axis correspond to the relative levels of  $\beta$ -galactosidase translated from SD\*-lacZ (control) mRNA by each of the mutant ribosomes (as indicated). Data represent the mean  $\pm$  SEM from three or more independent experiments. Values on the rightward axis reflect the missense error rate, calculated as the level of active  $\beta$ -galactosidase produced

from SD\*-lacZ (GAA 461 GAT) divided by that from SD\*-lacZ (control). For the wild-type specialized ribosomes, this quotient was  $0.0013 \pm 0.00008$ . The data shown correspond to the normalized quotient of two mean  $\pm$  SE from three or more independent experiments. Mutations analyzed include those identified in the screens and those engineered. Prefixes “ins” and “ $\Delta$ ” denote insertion and deletion, respectively.

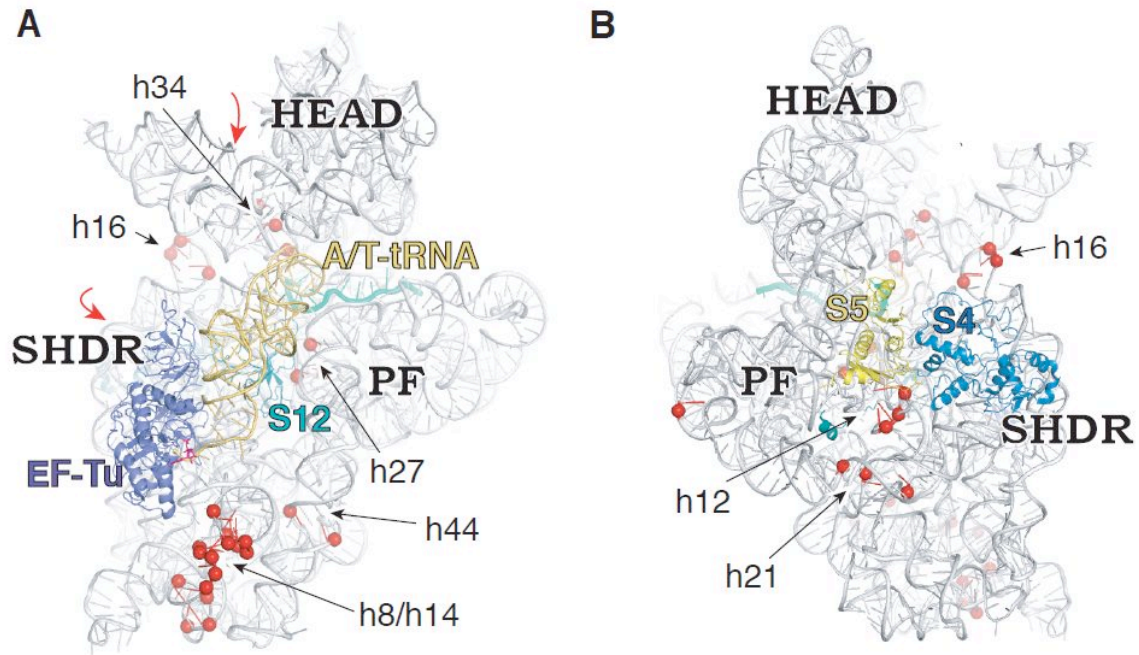


**Figure 4.** Where the mutations map. An overview of the locations of the mutations (depicted in red throughout) on the tertiary structure of 16S rRNA (PDB 2WRN) viewed from the interface (A) and solvent (B) perspective. Large red arrows in panel A indicate movements of 30S head and shoulder (SHDR) domains with respect to the platform (PF) during domain closure.



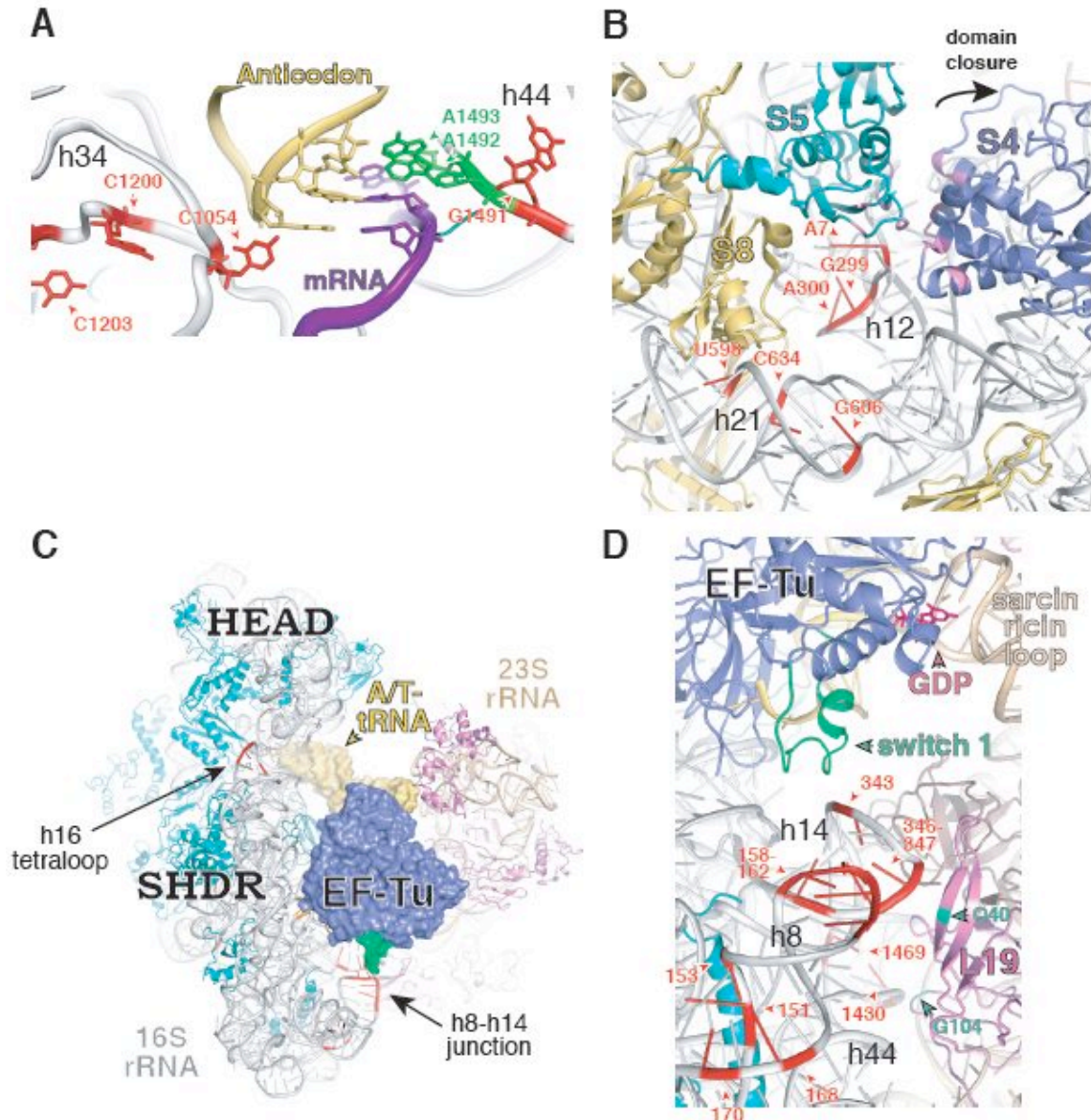


**Figure 5.** (A) View of the 30S A site (PDB 2WRN) showing locations of mutations in the vicinity. (B) Solvent view of the 30S subunit (PDB 2AVY) showing mutations found in h12 and h21. (C) Cryo-EM reconstruction of the ternary complex bound to the 70S ribosome in the presence of kirromycin (Protein Data Bank [PDB] 3FIH and 3FIK). The modeled switch 1 motif of EF-Tu is shown in green near the h8-h14 junction. (D) Closer view of the complex shown in panel C, showing locations of mutations found in h8, h14, and h44 (PDB 3FIH and 3FIK).

## Rates of GTP hydrolysis

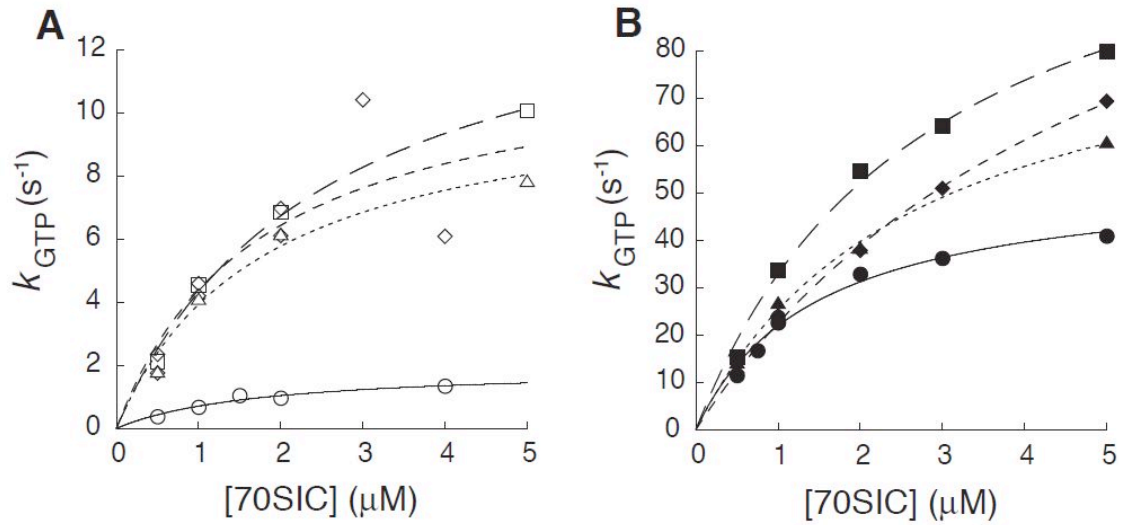


**Figure 6.** Effects of mutations in helices h8 and h14 on initial selection. 70S initiation complexes (70SIC) programmed with either cognate UUU (closed symbols) or near-cognate CUU (open symbols) in the A site were rapidly mixed with EF-Tu•[ $\gamma$ - $^{32}\text{P}$ ]GTP•Phe-tRNA<sup>Phe</sup>, and rates of GTP hydrolysis were determined. Wild type indicated by □/□ and solid lines; G347U, □/□ and long dashed lines; h14Δ2, ◆/◇ and medium dashed lines; and h8Δ3, □/△ and short dashed lines. (A) Apparent rates for near-cognate tRNA and (B) cognate tRNA plotted versus [70SIC].

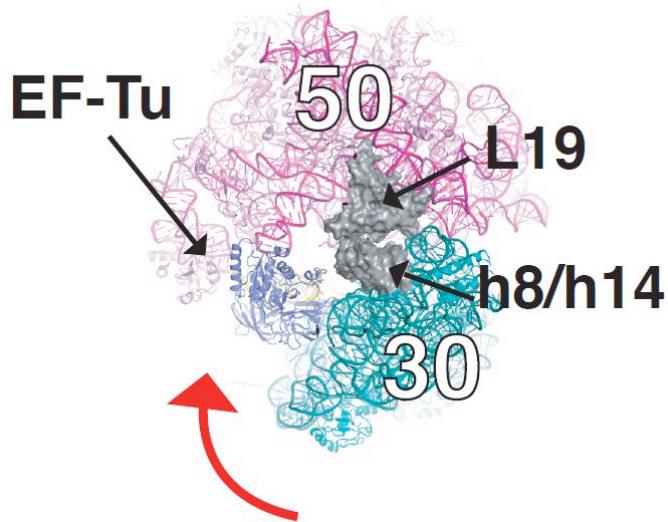


**Figure 7.** Proposed role for helices h8 and h14 in negatively regulating EF-Tu GTP hydrolysis. Red arrow indicates movement of the 30S shoulder during domain closure. EF-Tu primarily binds to the 30S subunit, but contacts the 50S subunit during GTP hydrolysis. Bridge B8, formed by h8/h14 and protein L19 (Grey) is positioned to resist the movement of the 30S shoulder relative to the 50S subunit, increasing the energy barrier to domain closure and increasing the stringency of the initial selection phase.

**Table 1.**

The Standard Genetic Code														
Second Position Nucleotide Base														
		U		C		A		G						
First Position Nucleotide Base	U	UUU	Phe	UCU	Ser	UAU	Tyr	UGU	Cys	U				
		UUC		UCC		UAC		UGC				C		
		UUA	Leu	UCA		UAA	UGA	Stop	A					
		UUG		UCG		UAG	UGG						Trp	G
	C	CUU	Leu	CCU	Pro	CAU	His	CGU		Arg	U			
		CUC		CCC		CAC		CGC				C		
		CUA		CCA		CAA	Gln	CGA	A					
		CUG		CCG		CAG		CGG					G	
	A	AUU	Ile	ACU	Thr	AAU	Asn	AGU		Ser	U			
		AUC		ACC		AAC		AGC				C		
		AUA		ACA		AAA	Lys	AGA	A					
		AUG		ACG		AAG		AGG					G	
	G	GUU	Val	GCU	Ala	GAU	Asp	GGU		Gly	U			
		GUC		GCC		GAC						GGC		
		GUA		GCA		GAA		Glu	GGA			A		
		GUG		GCG		GAG			GGG				G	
Third Position Nucleotide Base														
		U		C		A		G						
U		U		C		A		G		U				
C		C		G		A		G		C				
A		A		A		A		G		A				
G		G		G		A		G		G				

**TABLE 2** Mutations in 16S rRNA that increase misreading of sense and stop codons

Mutation	Location	Number of independent isolates in each suppressor screen <sup>a</sup>	
		Missense <sup>b</sup>	Nonsense <sup>c</sup>
A7G	5' end	2	0
A151G	h8	1	4
C153U	h8	1	0
G158A	h8	1	0
G159A	h8	6	0
A160G	h8	9	3
A161G	h8	8	3
A162G	h8	1	0
G168A	h8	2	0
U170A	h8	1	0
G299A	h12	15	5
A300G	h12	1	0
U343C	h14	1	0
ins345A <sup>d</sup>	h14	0	1
G346A	h14	3	0
G347A	h14	5	3
G347U	h14	1	0
ΔG348	h14	0	1
A349G	h14	1	0
ΔU420	h16	1	0
G423A	h16	0	1
G424A	h16	1	0
U598C	h21	1	0
G606A	h21	0	1
C634U	h21	4	6
G661A	h22	1	0
G886A	h27	1	0
U911C	h27	1	1
C1054U	h34	0	4
C1200U	h34	1	16
C1203U	h34	3	0
A1430G	h44	4	0
C1469U	h44	1	0
G1491A	h44	0	4

ins indicates insertion; Δ, deletion.

<sup>a</sup>Isolates were only considered independent if they originated from separate preparations of mutagenized pKF207.

<sup>b</sup>In this case, codon 461 of *lacZ* was changed from GAA to GAT. Production of active β-galactosidase requires misreading of GAU by Glu-tRNA.

<sup>c</sup>In this case, codon 585 of *lacZ* was changed from TGG to TGA. Production of active β-galactosidase requires read-through of UGA.

<sup>d</sup>Insertion of A after C345.